

ON THE NUMERICAL SOLUTION OF STURM-LIOUVILLE EQUATIONS IN THE THEORY OF MOLECULAR DIFFUSION

M. W. EVANS and S. J. ABAS*

Department of Physics, University College of North Wales, Bagnor, Gwynedd
* Department of Applied Mathematics, University College of North Wales, Bangor

(Received 4 February 1985)

ABSTRACT

The Sturm-Liouville equation from Budo's Theory of diffusion in the presence of potential wells is solved numerically for the normalised complex polarisability across the complete range of well depth (Vo/kT) from zero to effectively infinite. For Vo/kT = 0 and Vo/kT = ∞ a Debye process is recovered, in excellent agreement with available analytical limits. At intermediate Vo/kT the original Debye process for Vo/kT (free diffusion) is supplemented by a further loss process on the high frequency side. The numerical method used allow us to investigate the origin of this process in terms of the eigenvalues and eigenfunctions of the original Sturm-Liouville equation.

INTRODUCTION

Recently, the Budo theory [1,2] of interacting dipoles on a diffusing molecule has been considered again by W.T. Coffey and co-workers [3] in the context of the theory of the itinerant oscillator [4,5]. This analysis leads to an interesting numerical problem [6] involving the Sturm-Liouville equation:

$$Z_{\lambda}'' + (\lambda + \phi'(\theta) - \phi^2(\theta))Z_{\lambda} = 0 \tag{1}$$

$$\phi(\theta) = \frac{V'}{2kT} ; V = -\mu_1\mu_2 \cos \theta$$
$$\equiv -V_0 \cos \theta$$

Equation (1) is insoluble analytically, except in well-defined limits and the purpose of this paper is to provide the numerical solution for the complete

range of potential energy V_0 , the well-depth parameter. In eqn (1), Z_λ are eigenfunctions and λ eigenvalues of the Sturm-Liouville equation. The differentiation in eqn. (1) is with respect to the variable θ . μ_1 and μ_2 are the two interacting dipole moments. Results are given in terms of the complex polarisability in the range $V_0 = 0$ (free diffusion) to $V_0 \rightarrow \infty$, where the dipole-dipole interaction is so strong that the two diffusing dipoles are locked.

COMPUTATION

The Sturm-Liouville equation (1) was solved with a numerical method developed by Hargrave and Pryce [7,8] and implemented [3,6] in earlier work on the original Budo model. The numerical algorithm provides eigenvalues and eigenfunctions of any self-adjoint Sturm-Liouville system using a shooting method. The numerical method is found by shooting forward from a point $x = a$ and backward from a point $x = b$ to a matching point $x = c$. A relative scaling method is used to improve the numerical behaviour. The eigenvalues are computed with an absolute error (recorded after the symbol \pm in the tables of this paper). The true uncertainty in the eigenvalues is rarely more than twice, or less than a tenth, of this estimation.

The eigenfunction for a given eigenvalue is computed with a Prufer transform, upon which the numerical method is based. The method is now available as the Numerical Algorithms Group routine DO2KEF and is described in detail in their literature [9]. This routine outputs eigenfunctions at unequally spaced mesh points θ . Further analysis to provide normalised complex polarisability curves involves several numerical integrations over the eigenvalues as described in the literature [3]. For the problem posed by Budo, this requires seven separate numerical integrations for each eigenfunction with the specialised Numerical Algorithm Group routine DOLGAF, and therefore careful control of uncertainty. The end result of these integrations are the weighting factors recorded in the tables below. Where the weighting factors become very small, the mesh $Z(\theta)$ is no longer fine enough for satisfactory error control of the numerical integrations, and this is marked with an asterisk in the tables.

BOUNDARY VALUES

It is essential to define the boundary values correctly for a physically meaningful outcome of our Sturm-Liouville problem. It is not always obvious what these boundary values are, and the following method has been adopted for

their definition.

i) It has been assumed that the eigenfunction $Z(\theta)$ vanishes at the boundary points $\theta=\theta_1$ and $\theta=\theta_2$.

ii) These boundary points have been chosen in such a way that when the potential term in the Sturm-Liouville equation vanishes, i.e. when the equation reduces to:

$$Z_\lambda'' + \lambda Z_\lambda = 0 \quad (2)$$

the eigenvalues λ are integers. The integral eigenvalues of eqn. (2) follow the series 1,4,9,16,..... as shown in the tables. In order to satisfy this condition, the boundary conditions for the Budo problem (eqn. (1)) must be:

$$Z_\lambda(-\pi/2) = Z_\lambda(\pi/2) = 0 \quad (3)$$

By carefully controlling the absolute error in the eigenvalues and relative error in the various numerical integrations of the eigenfunctions, it is possible to produce a solution in terms of complex polarisability accurate to $\pm 0.1\%$ or better. Therefore, the solution of any Fokker-Planck [4,5] or Chandrasekhar [6] diffusion equation reduces to a Sturm-Liouville equation and therefore to an eigenvalue problem.

The numerical solutions were found for this work using the CDC 7600 computer of U.M.R.C.C. via remote link to the Bangor (U.N.C.W.) computer laboratory. Depending on the value of parameter such as V_0/kT , a complete polarisability curve (a sum of up to fifteen integrated eigenfunctions - 105 numerical integrations and 15 separate iterative solutions of the Sturm-Liouville equation) could be generated in about eleven decimal seconds of 7600 CPU time.

DISCUSSION OF TABULATED EIGENVALUES AND WEIGHTING FACTORS

Budo Model of Interacting Dipoles in a Diffusing Molecule [1,2]

The eigenvalues $\lambda_0, \lambda_1, \dots, \lambda_n$ as functions of the interaction energy V_0/kT are tabulated in table (1), together with the relaxation times τ_n defined by eqn. (1) for $\zeta_1/\zeta = 0.5$ and $2\zeta_1/kT = 10^{-8}$ sec, where ζ_1 and ζ are friction coefficients [1,2] on the dipole group and whole molecule respectively. In the limit $V_0/kT = 0$ the eigenvalues are described by the quadratic series $(n+1)^2$, $n = 0, 1, 2, \dots$. As V_0/kT increases, the zeroth

TABLE 1

λ_n	V_0/kT					
	0	0.01	0.1	1.0	5.0	10.0
n=0	1.000 $\pm 7.9 \times 10^{-5}$	0.990 $\pm 6.2 \times 10^{-5}$	0.904 $\pm 6.2 \times 10^{-5}$	0.324 $\pm 6.2 \times 10^{-5}$	0.001 $\pm 8.5 \times 10^{-5}$	0.000 $\pm 5 \times 10^{-5}$
1	4.000 $\pm 2.5 \times 10^{-4}$	4.000 $\pm 2.5 \times 10^{-4}$	4.007 $\pm 2.5 \times 10^{-4}$	4.662 $\pm 2.9 \times 10^{-4}$	17.421 ± 0.001	37.806 ± 0.0030
2	9.000 $\pm 5.6 \times 10^{-4}$	9.000 $\pm 5.6 \times 10^{-4}$	9.006 $\pm 5.6 \times 10^{-4}$	9.611 $\pm 6.0 \times 10^{-4}$	26.832 ± 0.0017	69.788 ± 0.0046
3	16.000 ± 0.001	16.000 ± 0.001	16.005 ± 0.001	16.535 ± 0.001	30.651 ± 0.0019	70.547 ± 0.0043
4	25.000 ± 0.0016	25.000 ± 0.0016	25.005 ± 0.0016	25.522 ± 0.0018	37.970 ± 0.0024	71.402 ± 0.0059
5	36.000 ± 0.0023	36.000 ± 0.0023	36.005 ± 0.0023	36.514 ± 0.0023	49.409 ± 0.0031	96.204 ± 0.0077
6	49.002 ± 0.0031	49.002 ± 0.0031	49.008 ± 0.0031	49.511 ± 0.0031	62.211 ± 0.0039	110.687 ± 0.0069
7	64.003 ± 0.004	64.000 ± 0.0040	64.0030 ± 0.004	64.507 ± 0.0040	76.998 ± 0.0048	120.266 ± 0.0075
8	81.001 ± 0.0051	81.001 ± 0.0051	81.005 ± 0.0051	81.008 ± 0.0051	93.891 ± 0.0059	134.937 ± 0.0084
9	100.004 ± 0.0063	99.994 ± 0.0062	100.005 ± 0.0063	100.507 ± 0.0063	112.818 ± 0.0098	153.724 ± 0.0096
10	121.003 ± 0.0076	120.999 ± 0.0076	120.999 ± 0.0076	121.509 ± 0.0076	133.762 ± 0.0084	174.107 ± 0.011

$10^8 \tau_n$	V_0/kT					
	0	0.01	0.1	1.0	5.0	10.0
n=0	0.333	0.334	0.334	0.430	0.500	0.500
1	0.167	0.167	0.166	0.150	0.051	0.025
2	0.091	0.091	0.091	0.086	0.035	0.014
3	0.056	0.056	0.056	0.054	0.031	0.014
4	0.037	0.037	0.037	0.036	0.025	0.014
5	0.026	0.026	0.026	0.026	0.019	0.010
6	0.020	0.020	0.020	0.019	0.016	0.009
7	0.015	0.015	0.015	0.015	0.013	0.008
8	0.012	0.012	0.012	0.012	0.010	0.007
9	0.010	0.010	0.010	0.010	0.009	0.006
10	0.008	0.008	0.008	0.008	0.007	0.006

$$y(-\pi/2) = y(\pi/2) = 0$$

$$\zeta_1/\zeta = 0.5; \quad 2\zeta_1/kT = 10^{-8} \text{ sec}$$

TABLE 2

I_λ	$\frac{V_0}{kT}$ 0.00	0.01	0.10	1.00	5.00	10.00
$\lambda=0$	2.146 ± 0.006	2.158 $\pm 6 \times 10^{-4}$	2.205 ± 0.006	2.897 ± 0.004	3.640 ± 0.005	3.745 ± 0.004
1	6.6×10^{-5} $\pm 2 \times 10^{-4}$	6.1×10^{-5} $\pm 2 \times 10^{-4}$	2.9×10^{-5} $\pm 6 \times 10^{-5}$	2.2×10^{-5} $\pm 8 \times 10^{-4}$	4.3×10^{-7} ± 0.03	4.7×10^{-6} ± 0.01
2	1.8×10^{-4} ± 0.002	4.3×10^{-4} $\pm 3 \times 10^{-3}$	0.0059 $\pm 9.5 \times 10^{-3}$	0.29 ± 0.06	1.00 ± 0.006	0.695 ± 0.007
3	0.02 ± 0.07	0.015 ± 0.07	0.002 ± 0.005	3.6×10^{-5} ± 0.001	2.4×10^{-8} ± 0.01	2.4×10^{-3} ± 0.01
4	*	*	*	0.047 ± 0.010	0.56 ± 0.10	0.66 ± 0.007
5	*	*	*	0.0014 ± 0.01	1.9×10^{-6} ± 0.05	6.3×10^{-8} ± 0.002
6	*	*	*	0.002 ± 0.002	0.16 ± 0.02	0.238 ± 0.002
7	*	*	*	*	2.6×10^{-6} ± 0.02	3.0×10^{-6} ± 0.09
8	*	*	*	*	0.034 ± 0.055	0.126 ± 0.001
9	*	*	*	*	7.6×10^{-6} ± 0.06	2.5×10^{-5} ± 0.30
10	*	*	*	*	0.0049 ± 0.03	0.0447 ± 0.01
11	*	*	*	*	1.0×10^{-4} ± 0.04	2.8×10^{-6} ± 0.04
12	*	*	*	*	9.8×10^{-4} ± 0.04	0.0151 ± 0.002
13	*	*	*	*	1.4×10^{-4} ± 0.03	1.4×10^{-5} ± 0.21
14	*	*	*	*	3.1×10^{-5} ± 0.05	0.0041 ± 0.03

The Weighting Factors and Estimated Uncertainties (After seven numerical integrations) Inc Eqn

$$\mu_1 = \mu_2 = 1.0$$

B.C.'s $-\pi/2$ to $\pi/2$

Note that $I_\lambda = 0$; $\lambda = 2n + 1$

* Mesh-nets not fine enough for accurate integration. I_λ very small

order eigenvalue $\lambda_0 \rightarrow 0$ but all the others increase. The effect of this behaviour on the relaxation times τ_n is summarised in table (1). (The times are defined by repeated numerical integration as described [3] in the literature). The relaxation time τ_0 gradually increases as a function of V_0/kT but all the others (i.e. $n = 1, 2, \dots$) decrease. As $V_0 \rightarrow \infty$, therefore there remains a single, finite relaxation time τ_0 only; i.e. the complex polarisability curve becomes once more Debye type [3,4] because the two dipoles are locked together and diffuse as a single entity. This is in agreement with theoretical predictions, because the Sturm-Liouville equation (1) reduces to an analytically soluble Hermite equation [5] in the limit $V_0/kT \rightarrow \infty$.

Table (2) records the weighting factors I_λ built up by seven numerical integrations from the eigenvalues of eqn. (1). These integrals are fully described in the literature [3,6]. In the limit $V_0/kT \rightarrow 0.0$ only the first factor, I_0 , is significant, because the dipoles in this limit diffuse independently according to Debye's equation [4]. For all V_0/kT the odd weighting factors (i.e. for $n = 1, 3, 5, \dots$) vanish and we may restrict the problem to the case $n = 0, 2, 4, 6, \dots$. The factor I_2 rises to about 30% of I_0 at intermediate values of V_0/kT , but thereafter $I_{n+2}/I_n \rightarrow 0$ as $V_0/kT \rightarrow \infty$.

The complex polarisability from the Budo equation [1,2] is, finally, a sum over the even weighting factors and correlation times and the imaginary part, $\alpha''(\omega)$, is illustrated in fig. (1) normalised by $\sum_{\lambda} I_{\lambda}$.

DISCUSSION

It is clear from fig. (1) that as V_0/kT increases, a secondary loss process appears on the high frequency side of the $V_0/kT = 0$ curve. This loss process (or complex polarisability curve) is due to the fact that the diffusion of the two dipoles μ_1 and μ_2 is no longer independent. In the original model considered by Budo, the two dipoles μ_1 and μ_2 are those of two groups attached to the same diffusing molecule. (Experimentally [10], the process of internal rotation (e.g. of a CH_3O -group) could produce loss curves such as those in fig. (1)). However, it is interesting to note that the potential energy V_0 may originate in the interaction of two dipoles on independently diffusing molecules; the director potential of a nematogenic environment [11], from the equations governing the interaction between rotation and translation [12], and so on. The numerical methods developed to solve eqn. (1) therefore have a wide range of applicability. The general analytical form of the overall polarisability curve is (s is the Laplace variable:

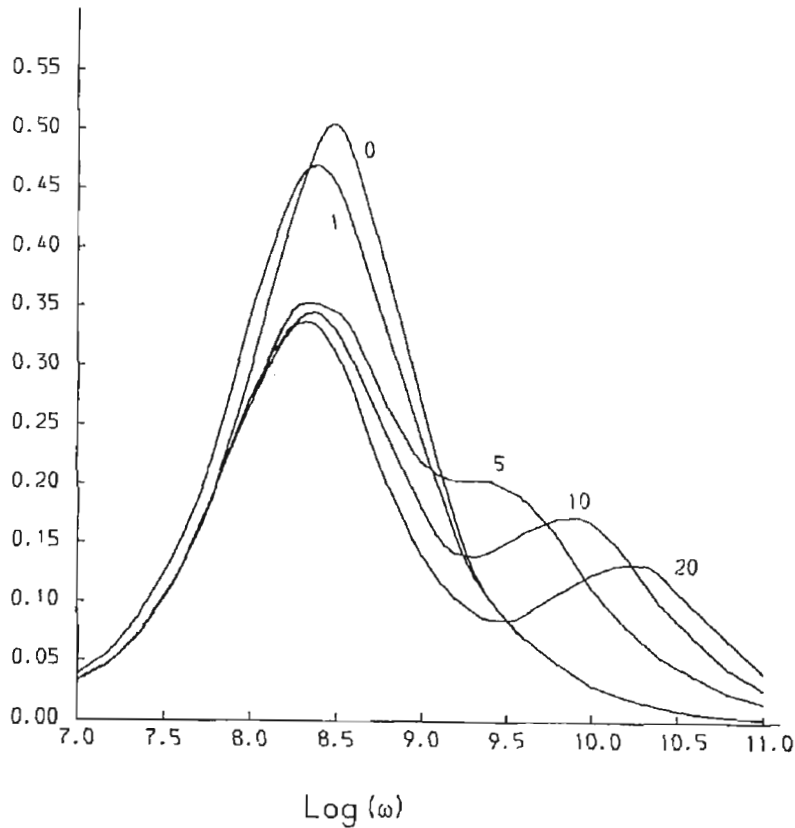
$\alpha''(\omega) / \alpha'(0)$


Fig. 1. Curves of normalised complex polarisability $\alpha''(\omega/\alpha'(0))$ vs. $\log_{10}(\omega)$ from the Budo theory behind eqn. (1). Each curve is marked with V_0/kT .

$$\begin{aligned}
 & a \langle \cos\theta_0 \cos\theta(t) \rangle \\
 & = \frac{\sum_{\lambda} \left| \int_0^{2\pi} \int_0^{2\pi} \cos\theta_0 \cos\theta(t) W(\theta_0) e^{-V(\theta)/2kT} Z_{\lambda}(\theta) Z_{\lambda}(\theta_0) d\theta d\theta_0 \right|}{\int_0^{2\pi} W(\theta) Z_{\lambda}^2(\theta) d\theta (s + \lambda \frac{kT}{\zeta})} \quad (4)
 \end{aligned}$$

$$\text{where } W(\theta) = \exp \left[-\frac{V_0}{kT} (1 - \cos\theta) \right]$$

i.e. there is a distribution of relaxation times as in fig. (1).

Analytical checks on the accuracy of the numerical results of fig. (1) can be made as follows. The analytical difference between the relaxation times in the limit $V_0 \rightarrow 0$ (τ_{free}) and $V_0 \rightarrow \infty$ (τ_{hind}) is given by [5]:

$$\frac{1}{\tau_{free}} - \frac{1}{\tau_{hind}} = \frac{kT}{2\zeta_1} \quad (5)$$

and the ratio by [5]:

$$\frac{\tau_{hind}}{\tau_{free}} = \frac{\omega_{max}^{free}}{\omega_{hind}} = \frac{2(1 + \zeta_1/\zeta)}{(1 + 2\zeta_1/\zeta)} \quad (6)$$

The parameters used in fig. (1) were $\mu_1 = \mu_2 = 1.0$, $\zeta_1/\zeta = 0.5$; $2\zeta_1/kT = 10^{-8}$ and produce the analytical result:

$$\log_{10}(\omega_{free}) - \log_{10}(\omega_{hind}) = 0.176$$

from eqn. (6).

From fig. (1), however, for $V_0/kT = 0$, $\log_{10}(\omega_{free}) = 8.48$; for $V_0/kT = 20.0$, $\log_{10}(\omega_{hind}) = 8.31$, i.e. a difference of 0.17(0), which is already in satisfactory agreement with the limiting ($V_0/kT \rightarrow \infty$) analytical value of 0.176. This is an important verification that numerical errors have been kept well within the bounds of acceptability, bearing in mind that each loss curve of fig. (1) requires up to 15 separate numerical solutions of the Sturm-Liouville equation and therefore up to 105 numerical integrations over unequally spaced mesh-points, with subsequent accumulation of numerical uncertainty.

Another check is possible - on the normalised amplitude of the two loss curves of fig. (1). The analytical results [5] provide:

$$\tau_{hind} = \left[\frac{kT}{2\zeta_1} \left(1 + 2 \frac{\zeta_1}{\zeta} \right) \right]^{-1} ; \quad (7)$$

$$\tau_{free} = \left[\frac{kT}{\zeta_1} \left(1 + \frac{\zeta_1}{\zeta} \right) \right]^{-1} \quad (8)$$

The normalised maximum amplitude of the curve $\alpha''(\omega)/\alpha'(0)$ of fig. (1) is given by:

$$\frac{\alpha''(\omega)}{\alpha'(0)} = \sum_{\lambda} \frac{I_{\lambda} \omega \tau_{\lambda}}{1 + \omega^2 \tau_{\lambda}^2} / \sum_{\lambda} I_{\lambda} \quad (9)$$

TABLE 3

$\gamma = \frac{\mu E}{RT}$	0.01	0.10	1.00	5.00	10.00	20.00	50.000
$\frac{\lambda}{n}$							
n=0	1.000 $\pm 8.1 \times 10^{-5}$	1.002 $\pm 6.3 \times 10^{-5}$	1.165 $\pm 7.5 \times 10^{-5}$	4.355 $\pm 2.7 \times 10^{-4}$	9.451 $\pm 7.3 \times 10^{-4}$	19.508 ± 0.0018	49.547 ± 0.0031
1	4.000 $\pm 2.5 \times 10^{-4}$	4.001 ± 0.00026	4.134 $\pm 2.6 \times 10^{-4}$	7.663 $\pm 4.8 \times 10^{-4}$	17.637 ± 0.0011	37.866 ± 0.0018	97.951 ± 0.0062
2	9.000 $\pm 5.6 \times 10^{-4}$	9.001 $\pm 5.6 \times 10^{-4}$	9.129 $\pm 7.7 \times 10^{-4}$	12.352 ± 0.0015	24.051 ± 0.0048	55.036 ± 0.0048	145.406 ± 0.011
3	16.000 ± 0.0010	16.001 ± 0.001	16.127 ± 0.001	19.250 ± 0.0012	30.067 ± 0.0019	70.813 ± 0.0049	191.631 ± 0.0083
4	25.000 ± 0.0016	25.001 ± 0.0016	25.127 ± 0.0016	28.205 ± 0.0018	38.431 ± 0.0024	84.840 ± 0.0053	236.871 ± 0.017
5	36.000 ± 0.0023	36.001 ± 0.0023	36.127 ± 0.0023	39.180 ± 0.0024	49.134 ± 0.0031	96.410 ± 0.0060	280.689 ± 0.015
6	49.002 ± 0.0031	49.002 ± 0.0031	49.127 ± 0.0031	52.166 ± 0.0033	61.962 ± 0.0039	106.630 ± 0.0067	323.501 ± 0.022
7	64.003 ± 0.0040	64.004 ± 0.002	64.126 ± 0.004	67.158 ± 0.0042	76.853 ± 0.0048	119.426 ± 0.0075	346.686 ± 0.014
8	81.001 ± 0.0051	81.002 ± 0.0051	81.124 ± 0.0051	84.152 ± 0.0053	93.779 ± 0.0059	135.157 ± 0.0084	404.662 ± 0.0030
9	100.005 ± 0.0063	100.008 ± 0.0063	100.123 ± 0.0063	103.149 ± 0.0086	112.727 ± 0.0070	153.318 ± 0.0096	442.986 ± 0.024
10	121.003 ± 0.0076	121.002 ± 0.0076	121.123 ± 0.0076	124.142 ± 0.0078	133.687 ± 0.0084	173.720 ± 0.011	479.765 ± 0.038
11	144.000 ± 0.009	144.001 ± 0.009	144.122 ± 0.009	147.140 ± 0.0092	156.659 ± 0.0098	196.277 ± 0.012	514.592 ± 0.033
12	169.000 ± 0.011	169.001 ± 0.011	169.133 ± 0.011	172.139 ± 0.011	181.637 ± 0.011	220.934 ± 0.014	547.380 ± 0.047
13	195.998 ± 0.012	196.000 ± 0.012	196.136 ± 0.012	199.110 ± 0.012	208.619 ± 0.013	247.664 ± 0.015	577.569 ± 0.036
14	225.001 ± 0.014	225.00 ± 0.014	225.128 ± 0.014	228.111 ± 0.014	237.598 ± 0.015	276.447 ± 0.017	604.325 ± 0.052
15	255.999 ± 0.016	255.998 ± 0.016	256.121 ± 0.016	259.148 ± 0.016	268.598 ± 0.017	307.270 ± 0.019	626.913 ± 0.039

$$\frac{d^2 y}{dx^2} + \left| \lambda - \frac{\gamma^2}{8} + \frac{\gamma}{2} \cos x + \frac{\gamma^2}{8} \cos(2x) \right| y = 0$$

with $y(0) = 0$; $y(\pi) = 0$

and in the limit $V_0/kT \rightarrow 0.0$, there is only one eigenvalue, equivalent to the weighting factor I_0 . It is then easy to see that the maximum of $\alpha''(\omega)/\alpha'(0)$ is 0.5, because $\omega\tau_0 = 1$ at this frequency. The numerical result of figure (1) for V_0/kT is 0.500.

Finally, in the "locked-in limit" of $V_0/kT \rightarrow \infty$, there is, theoretically, an infinite number of correlation times, each with its own weighting factor I_λ . (This pattern begins to emerge in table (2) for $V_0/kT = 10.0$). In this case:

$$\left| \frac{\alpha''(\omega)}{\alpha'(0)} \right|_{\max} = \frac{0.5 I_0}{\sum_{\lambda} I_{\lambda}} \quad (10)$$

The intensity of the normalised complex polarisability curve therefore decreases with respect to the intensity in the limit $V_0/kT = 0$. This is again in agreement with the results from the computer (fig. (1), and tables (1) and (2)).

Another Sturm-Liouville system of importance which occurs in itinerant oscillator theory is [5] :

$$\frac{d^2 y}{dx^2} + \left[\lambda - \frac{\gamma^2}{8} + \frac{\gamma}{2} \cos x + \frac{\gamma^2}{8} \cos (2x) \right] y = 0 \quad (11)$$

with boundary conditions $y(0) = 0$; $y(\pi) = 0$ and the numerical methods developed by Hargrave and Pryce [7-9] produce the eigenvalues λ of table (3) for this system, as a function of a dipole-electric field potential ($\gamma = \mu E/kT$). It can be seen that small differences in the structure of the Sturm-Liouville equation produce quite different eigenvalue patterns (cf eqn. (1); table 1; and eqn. (11); table (3)).

ACKNOWLEDGEMENTS

The University of Wales is thanked for a fellowship, and Dr. W.T. Coffey for the motivation for this work.

REFERENCES

- 1 A. Budo, Phys. Zeit, 39 (1938) 706.
- 2 A. Budo, J. Chem. Phys., 17 (1949) 686.
- 3 M.W. Evans, W.T. Coffey and J.D. Pryce, Chem. Phys. Lett., 63 (1979) 133.
- 4 M.W. Evans, G.J. Evans, W.T. Coffey and P. Grigolini, "Molecular Dynamics", Chapter 3, Wiley/Interscience, N.Y., (1982).
- 5 W.T. Coffey, M.W. Evans, and P. Grigolini, Chapters 3-6, Wiley/Interscience, N.Y., (1984).
- 6 M.W. Evans, Adv. Mol. Rel. Int. Proc., 15 (1979) 273.
- 7 B. Hargrave and J.D. Pryce, NPARAM: Report on Program to Solve the Multiparameter Sturm-Liouville Problem, Bristol Univ. Computer Science Dept., (1977).
- 8 J.D. Pryce, Inst. Maths. Applics., Numerical Analysis Newsletter, vol. 1, No 3 (1977).
- 9 N.A.G. Library, Routines DO2KEF and DO1GAF (FORTRAN).
- 10 N. Hill, W. Vaughan, A.H. Price and M. Davies, "Dielectric Properties and Molecular Behaviour", van Nostrand/Rheinhold, (1969).
- 11 ref. 4, Chapter 8, for example.
- 12 M.W. Evans, Phys. Rev., 30A (1984) 2062.